

Figure 1. Generalized surface geology map of Sabine Peninsula (after Harrison, 1994).

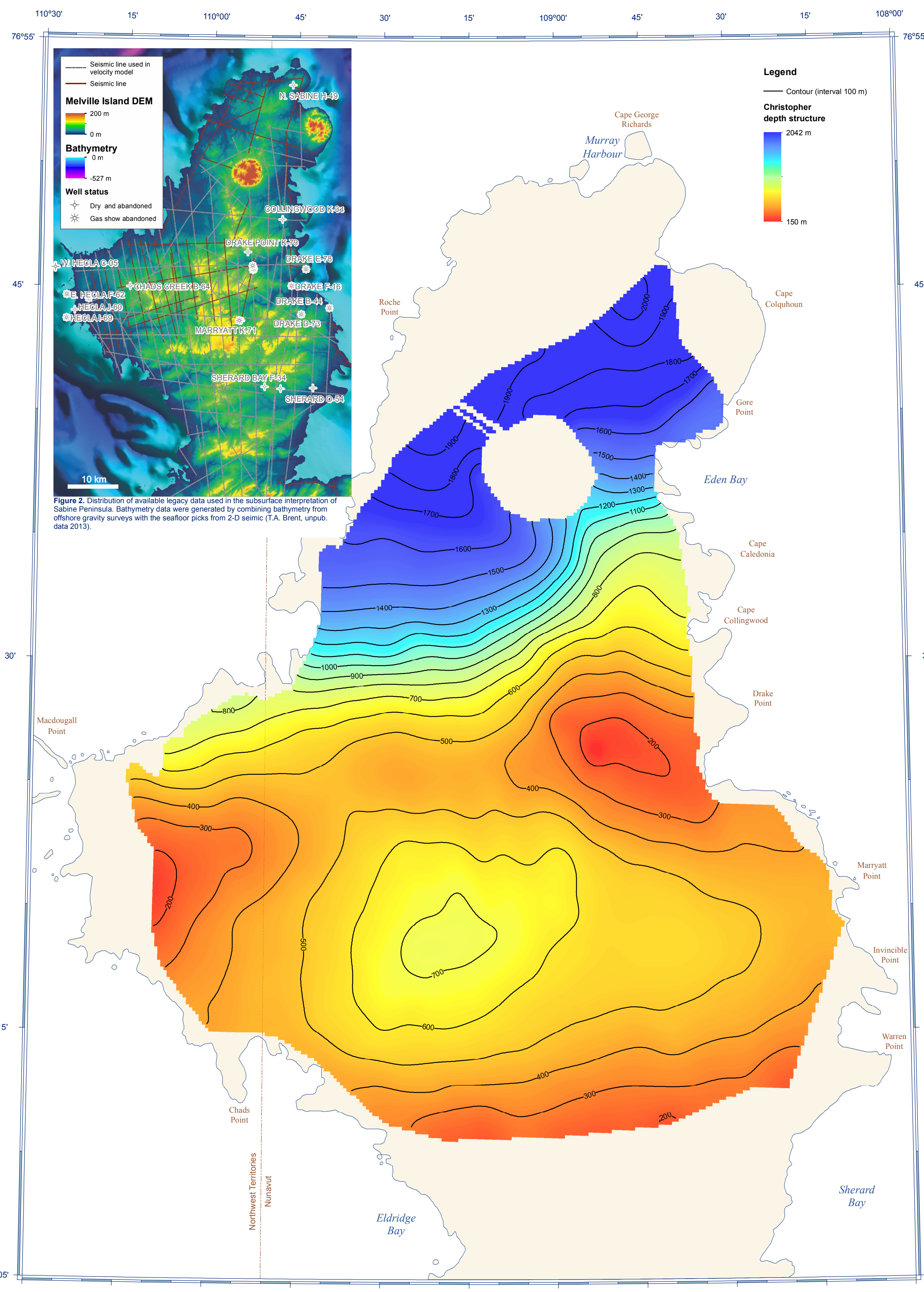


Figure 2. Distribution of available legacy data used in the subsurface interpretation of Sabine Peninsula.

INTRODUCTION
The time- and depth-structure maps presented herein are part of an eight-map series of the subsurface of Sabine Peninsula spanning the Early Permian through Early Cretaceous interval. These maps are the product of the application of modern geoscientific methods of processing and interpretation to a suite of legacy seismic-reflection data from onshore Sabine Peninsula (Melville Island, western Arctic). Processing errors may result from inadequate static corrections, inaccurate velocity analysis, and inappropriate parameter determination. More specifically to this data set, errors may have also been introduced by the velocity model and the ability to pick formation tops to seismic horizons. The velocity model represents an estimation of the velocity fluctuations for which the accuracy depends on the number of wells and the good fit between time picks and corresponding depths at the well locations. A regression analysis shows that time picks and their corresponding depths at the wells have a strong linear fit ($r = 0.98$), meaning that the use of time picks as the external drift in the kriging strategy is justified and producing a Newell-style, non-linear, uncertainty that increases with the distance between the well and any points where velocity is predicted exceeds the range of the varying expression of the spatial dependence between depth and time. In the present case, the range of the different horizons is between 5 km and 34 km. The ability to formation tops to seismic horizons relies on the successful use of well sonic and density logs, since it is the contrast between the product of these properties for two successive geological layers that generates reflections recorded in seismic exploration. Formation tops used in this study are from Dewing and Embry (2007), for which they mainly utilized gamma-ray logs to position the upper limit of the formations in depth. Thus errors may have been introduced by projecting the formation tops on seismic sections recorded in time.

REGIONAL SETTING
The Sabine Peninsula is located within the Sverdrup Basin in the Queen Elizabeth Islands of the western Arctic. The Sverdrup Basin extends for about 1300 km in a north-south-southwest direction and is up to 350 km wide. The basin contains up to 13 km of sedimentary strata (Embry and Beauchamp, 2008). The Sverdrup Basin is separated from the underlying Franklin Basin by an unconformity at the base of the Carboniferous strata. The Franklin Basin was extensively widespread during the Late Paleozoic to Early Mesozoic. The Sverdrup Basin is a major depocenter from the Carboniferous through the Paleogene (Embry and Beauchamp, 2008). The Sverdrup Basin succession was uplifted and deformed during the early Cenozoic Eurasian Orogeny. The surface geology of Melville Island is dominated by Lower Paleozoic strata of the Franklin Basin. The Sabine Peninsula is an exception to this, as surface strata are part of the Sverdrup Basin. The geology of the Sabine Peninsula consists of deformed Late Carboniferous to Paleocene sandstone, siltstone, shale, and minor amounts of carbonate. Additionally, evaporitic rocks are exposed in two diapirs on northern Sabine Peninsula—the Barrow and Colquhoun domes, which consist of deformed anhydrite and gypsum. The strata of the Sverdrup Basin succession on Melville Island were deformed into a series of folds, including the Murray Harbour syncline in the northern part of the peninsula and the Drake Point anticline and the Maryatt Point syncline to the south (Harrison, 1994) (Fig. 1). During a 1961 to 1965 phase of petroleum exploration, companies drilled 52 wells on Melville Island and surrounding waters (22 of which were on Sabine Peninsula) and acquired about 3,400 line-kilometers of seismic-reflection data (Fig. 2). Three separate gas fields were discovered in the Sabine Peninsula area: Drake Point, Hecla, and Roche Point. Feasibility studies for the development of the gas fields were conducted in the early 1980s; however, due to low gas prices and the lack of gas markets, the gas fields on Melville Island (and elsewhere in the Canadian Arctic) were not developed (Harrison, 1995).

SEISMIC DATA SET AND PROCESSING
Data access was obtained through a Memorandum of Understanding signed in 1997 by the Geological Survey of Canada (GSC), Panarctic Oils, the Arctic Islands Exploration Group, and the Northern Arctic Exploration Group venture parties. The data sets consist of original land seismic-reflection field tapes transcribed from 21-, 7-, and 9-track media. Data were collected using a dynamic charge of 20–30 kg per shot at about 20 m below the surface. Shot-point spacing ranged from 61 m to 300 m, the shorter spacing being used for most surveys. The majority of the seismic-reflection data were recorded using 48- or 96-channel systems. Channel stations were generally deployed using nine receivers spaced at about 8 m and station intervals varying from 50 m to 70 m. The common-midpoint multiplicity of the data sets range from single to 12-fold coverage. The most common recording length was 6 s. The processing consisted of three main stages: 1) principal component decomposition was used to remove both coherent and random noise, 2) data were migrated utilizing poststack Kirchhoff migration, and 3) seismic bandwidths were extended to increase vertical resolution (Claproot et al., 2011; Duchesne et al., 2012).

Velocity model
A 3-D velocity model was built using about 1300 km of linear seismic data (78 lines) and 13 wells spread over an area of about 2800 km² (Fig. 2). The velocity model was then used for poststack migration processing and to convert seismic horizon surfaces from time to depth. The primary assumption behind the velocity model is that the coherent high-amplitude reflections that were picked to build the model correspond to important acoustic impedance contrasts caused by significant and abrupt velocity changes. This assumption was confirmed by using seismic picks to well sonic logs (Duchesne et al., 2012). The geostatistical approach of kriging with an external drift (KED) was applied to both the reflection time of the picked seismic horizons and time-depth pairs derived from check shot data to compute the 3-D velocity field. Kriging interpolates values between the known positions based on weighted spatial correlations. The KED technique was specifically developed for the integration of seismic data into the kriging process where the number of wells is insufficient for the computation of adequate depth statistics (Haas and Dubrule, 1994). Hence, it uses the information provided by the time horizon picks to improve estimates where depth control is sparse. For seismic migration, root-mean squared (RMS) velocity values are first estimated by KED from time-to-depth conversion of seismic horizon surfaces mapped as important velocity boundaries (Duchesne et al., 2012). Then, once the approximate depths of the surfaces are known, the interval velocities (V_{ij}) for all time intervals delimited by two consecutive horizons is computed from:

$$V_{ij} = \frac{\Delta z_j}{\Delta t_j}$$

where Δz_j and Δt_j are the depth and time intervals between two successive horizons j . Once V_{ij} is obtained the RMS velocity (V_{rms}) is calculated using:

$$V_{rms} = \sqrt{\frac{\sum_{i=1}^N V_{ij}^2 \Delta t_i}{\sum_{i=1}^N \Delta t_i}}$$

in which N is the total number of horizons and Δt_i is the sum of all time intervals.

SEISMIC INTERPRETATION AND VISUALIZATION METHODS
Processed seismic lines were loaded into IRIS-Kingdom[®] seismic and geological interpretation software. Prominent seismic-reflection horizons, tied to well formation-top information, were manually correlated. Seed points were generated at seismic line intersections, thereby permitting the interpretation of adjacent lines. The map would benefit from a detailed structural interpretation; however, confidence of this interpretation is minimized due to minor vertical offsets (about 1.1 s) attributed to faulting and the large line spacing. Thus reflections are readily identified across faults despite offset. Time-structure maps of the key seismic horizons were computed using universal kriging. Universal kriging permits the interpolation of a nonstationary, random field by adding a term in the kriging equation that accommodates any linear trends present in a scattered point set (Chiles and Delhomme, 1999). Given that all picked horizons showed a strong linear trend for time versus depth over distance, universal kriging provided the best fit to the picked horizons. The map would benefit from a detailed structural interpretation; however, confidence of this interpretation is minimized due to minor vertical offsets (about 1.1 s) attributed to faulting and the large line spacing. Thus reflections are readily identified across faults despite offset. Time-structure maps of the key seismic horizons were computed using universal kriging. Universal kriging permits the interpolation of a nonstationary, random field by adding a term in the kriging equation that accommodates any linear trends present in a scattered point set (Chiles and Delhomme, 1999). Given that all picked horizons showed a strong linear trend for time versus depth over distance, universal kriging provided the best fit to the picked horizons.

TIME TO DEPTH CONVERSION
All time surfaces are converted to depth using the following procedure. First V_{ij} of the 3-D velocity model are calculated using the equation:

$$V_{ij} = \left[\frac{r^2 t_{i-1}^2 + t_{i-1}^2 - r^2 t_i^2 - t_i^2}{t_i - t_{i-1}} \right]^{1/2}$$

where r is the zero-offset arrival time of the i th reflection. Interval limits corresponded to seismic horizons that are picked and tied to geological interfaces. Then V_{ij} are extracted from the velocity model along picked horizons. Velocity maps are then computed using Universal kriging at a cell size of 250 m. Finally, the time-structure surfaces of the various seismic horizons are converted to depth (Z) using:

$$Z = \frac{V_{ij} t}{2}$$

Because the depth-conversion process is a function of the velocity model, the lateral extent of depth maps is confined to the lateral extent of the model. The final depth-structure maps were imported into ArcGIS for visualization using the Arc extension Team-GIS Kriging.

DESCRIPTIVE NOTES

LEGEND
— Contour (interval 100 m)
— Seismic line used in velocity model
— Seismic line
Bathymetry (m)
Well status
Dry and abandoned
Gas show abandoned

UNCERTAINTY
Quantifying the uncertainty of seismic subsurface maps is difficult since several sources of data, each with their unique level of uncertainty, are used in the map generation. Sources of error may arise from limitations in acquisition, processing, and interpretation. Moreover, seismic data are collected remotely and the images they provide are derived from generalized mathematical and physical concepts. Constraints on the acquisition that increase the uncertainty include gaps in coverage because of obstacles to source and receiver deployment, and effect of direction of shooting on data quality (Sherriff and Geldart, 1995). Processing errors may result from inadequate static corrections, inaccurate velocity analysis, and inappropriate parameter determination. More specifically to this data set, errors may have also been introduced by the velocity model and the ability to pick formation tops to seismic horizons. The velocity model represents an estimation of the velocity fluctuations for which the accuracy depends on the number of wells and the good fit between time picks and corresponding depths at the well locations. A regression analysis shows that time picks and their corresponding depths at the wells have a strong linear fit ($r = 0.98$), meaning that the use of time picks as the external drift in the kriging strategy is justified and producing a Newell-style, non-linear, uncertainty that increases with the distance between the well and any points where velocity is predicted exceeds the range of the varying expression of the spatial dependence between depth and time. In the present case, the range of the different horizons is between 5 km and 34 km. The ability to formation tops to seismic horizons relies on the successful use of well sonic and density logs, since it is the contrast between the product of these properties for two successive geological layers that generates reflections recorded in seismic exploration. Formation tops used in this study are from Dewing and Embry (2007), for which they mainly utilized gamma-ray logs to position the upper limit of the formations in depth. Thus errors may have been introduced by projecting the formation tops on seismic sections recorded in time.

TIME- AND DEPTH-STRUCTURE DATA DISPLAY
The time- and depth-structure data shown on this map were gridded at a cell size of 250 m using Universal kriging. Each map presents a grid with a stretched color ramp at 20% transparency. Time contours, generated from the time-structure grids, are shown in black at 50 ms interval, whereas depth contours derived from the depth-structure grid are presented at 100 m intervals.

CHRISTOPHER MAP DESCRIPTIONS
The Early Cretaceous Christopher Formation consists of shale, chert, carbonate, and diatomites (Dewing and Embry, 2007; see also Fig. 3). The Christopher Formation is usually the youngest, or shallowest formation identified in wells on Sabine Peninsula, except where local exposures of the younger Hecla Formation have been sampled north of the Christopher Formation and where the formation can be separated into the Macquogill Point and Invinible Point members (Dewing and Embry, 2007). Formation-top data indicate that the Christopher Formation is underlain exclusively by the Hecla Formation. Where the Christopher Formation reflection was correlated to formation-top data, the reflection was located below the top of the Christopher Formation and above the Walker Island Member of the Invinible Formation. The reflection was therefore determined to represent a prominent reflection in the middle of the Christopher Formation (Brake et al., 2012). The mapped Christopher Formation reflection extends from the narrowest point of the peninsula near Eldridge and Shearby bays to north of the Barrow Dome, and falls slightly short of covering the entire width of the peninsula. The data gap west of Eden Bay marks the location of Barrow Dome. Two-way travel times of the Christopher Formation reflection increase northward from 38 ms to 1302 ms, or from 150 m to 2042 m. The slope of the horizon is generally less than 2°, but slopes up to 7° near Shearby and Shearby bays. The Barrow Dome, aligned roughly parallel to the axis of the Murray Harbour syncline. The primary dip azimuth of the horizon to the north with two exceptions: 1) when it crosses the Drake Point anticline and Maryatt Point syncline, and 2) the area of the northeast dip found north of the Murray Harbour syncline (Harrison, 1994).



Figure 3. Comparison of the wiggle plot, synthetic trace, stratigraphy, age, and formation-top data for the Chads Creek B-64 well.

ACKNOWLEDGMENTS
The authors would like to thank J. Dietrich and B. MacLean (GSC Calgary) for their technical reviews that improved the overall quality of the maps. IRIS is acknowledged for providing Kingdom 8.8 seismic interpretation software.

REFERENCES
Brake, V.I., Duchesne, M.J., and Brent, T.A., 2012. Preliminary results of shallow subsurface geological mapping, Sabine Peninsula, western Arctic Islands. Geological Survey of Canada, Current Research 2012-5, 17 p. doi:10.4095/293672.

Chiles, J.P. and Delfiner, P., 1999. Geostatistics: Modeling Spatial Uncertainty. Wiley Series in Probability and Statistics. Wiley, New York, 734 p.

Claproot, M., Duchesne, M.J., and Gougeon, E., 2011. A geostatistical approach to 2-D seismic velocity modelling. Geological Survey of Canada, Open File 7045, 21 p. doi:10.4095/295651.

Dewing, K. and Embry, A.F., 2007. Geological and geochemical data from the Canadian Arctic Islands, Part I: Stratigraphic logs from Arctic Islands' oil and gas exploration boreholes. Geological Survey of Canada, Open File 5442, 1 CD-ROM. doi:10.4095/22338.

Duchesne, M.J., Claproot, M., and Gougeon, E., 2012. Improving seismic velocity estimation for 2-D poststack time migration of regional seismic data using kriging with an external drift. The Leading Edge, v. 31, p. 1156–1166.

Embry, A. and Beauchamp, B., 2008. Sverdrup Basin, in: Sedimentary Basins of the World, (ed. K.J. Hill), Volume 5: The Sedimentary Basins of the United States and Canada, Elsevier, Amsterdam, The Netherlands, p. 451–471.

Harrison, J.C., 1994. Melville Island and adjacent smaller islands, Canadian Arctic Archipelago, District of Franklin, Northwest Territories. Geological Survey of Canada, Map 1544-A, scale 1:250 000. doi:10.4095/203877.

Harrison, J.C., 1995. Melville Island's salt-based fold belt, Arctic Canada. Geological Survey of Canada, Bulletin 472, 34 p. doi:10.4095/203578.

Haas, A. and Dubrule, O., 1994. Geostatistical inversion – a sequential method of stochastic reservoir modeling constrained by seismic data. First Break, v. 12, p. 961–969.

Sherriff, R.E. and Geldart, L.P., 1995. Exploration Seismology. Cambridge University Press, New York, 626 p.

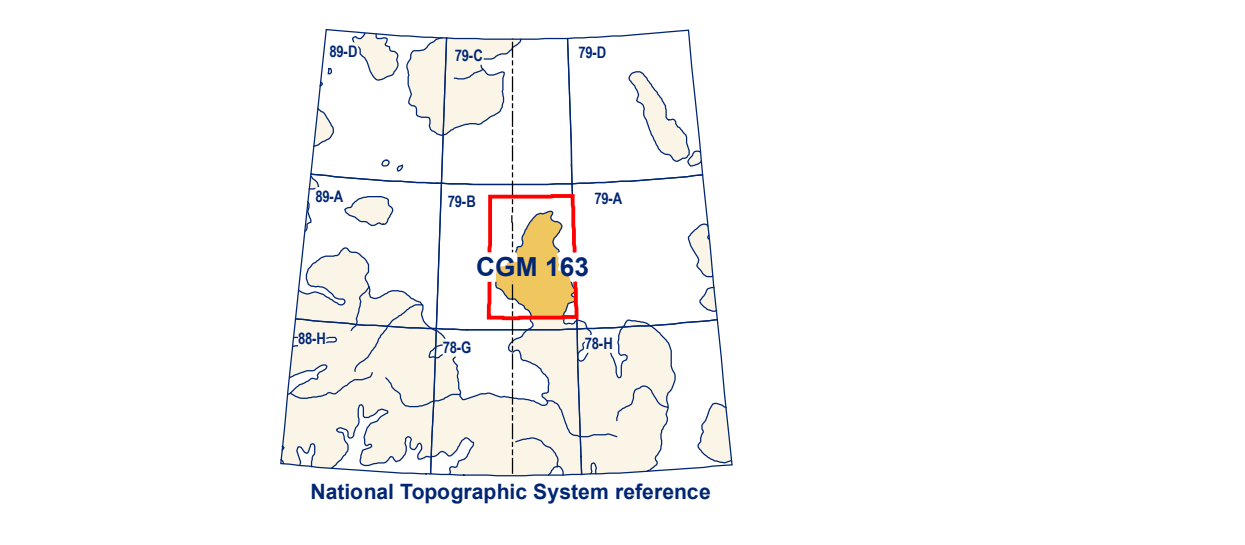
Recommended citation
Brake, V.I., Duchesne, M.J., Dewing, K., Claproot, M., Gougeon, E., and Brent, T.A., 2013. Time- and depth-structure map, Christopher Formation, Sabine Peninsula, Melville Island, Nunavut-Northwest Territories. Geological Survey of Canada, Canadian Geoscience Map 163, scale 1:200 000. doi:10.4095/293687.

Abstract
Sabine Peninsula of Melville Island was the subject of an oil and gas exploration boom from 1961 to 1965, during which time seismic-reflection data were collected and wells were drilled. As a result, the two largest conventional natural gas fields in Canada were discovered.

Résumé
La péninsule de Sabine de l'île de Melville a connu un boom d'exploration gazière et pétrolière entre 1961-1965 pendant lequel des données de sismique-réflexion furent acquises et des puits forés. Il en résultait la découverte des deux plus grands champs de gaz naturel conventionnels du Canada.

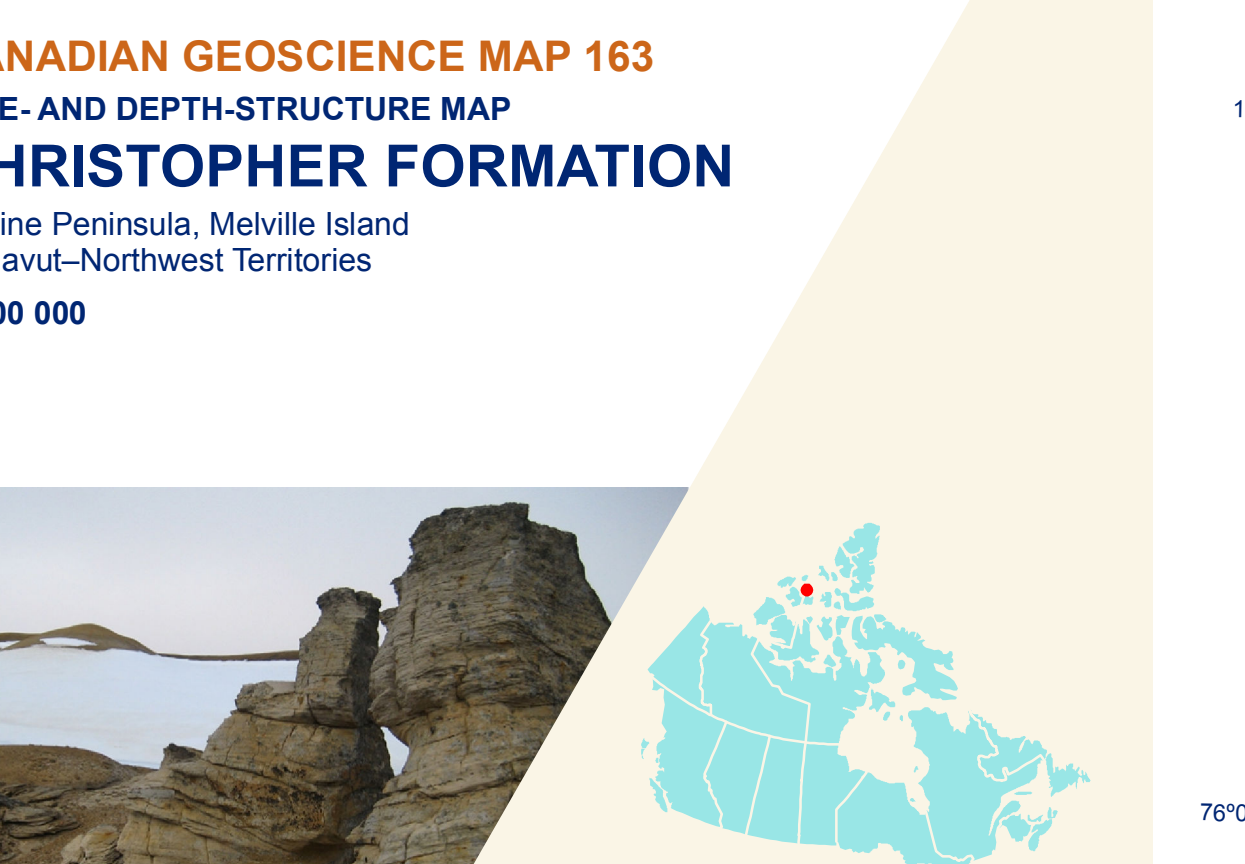
Seismic-reflection methods use sound waves to image the internal structure of the Earth. Waves are emitted at the surface before being reflected back to the surface via the surface and the interfaces between geological layers. Modern analysis methods were used to re-investigate existing seismic data. In doing so, eight seismic unit boundaries identified on seismic profiles in two-way time were correlated to the regional geological framework and gridded to provide subsurface maps. Each map approximates the structures preserved at that particular time or depth allowing the enhancement of the geological knowledge of Sabine Peninsula and better delineation of elements of the petroleum systems therein.

La sismique-réflexion utilise des ondes sonores pour imager la structure interne de la Terre. Les ondes sont émises au surface avant d'être réfléchies de nouveau vers la surface par des interfaces géologiques ou elles sont enregistrées. Des méthodes d'analyse modernes furent utilisées pour ré-investiguer des données sismiques existantes. Ainsi, huit limites d'unités sismiques identifiées sur les profils sismiques en temps de parcours aller-retour furent corrélées au cadre géologique régional et maillées afin de produire des cartes de la sous-surface. Chaque carte est une approximation des structures préservées à un certain temps ou une certaine profondeur nous permettant d'améliorer les connaissances géologiques de la péninsule de Sabine et de mieux délimiter les éléments des systèmes pétroliers s'y trouvant.



Catalogue No. M163-1163-2013E-PDF
ISBN 978-1-106-22821-7
doi:10.4095/293687
© Her Majesty the Queen in Right of Canada 2013

CANADIAN GEOSCIENCE MAP 163
TIME- AND DEPTH-STRUCTURE MAP
CHRISTOPHER FORMATION
Sabine Peninsula, Melville Island
Nunavut-Northwest Territories
1:200 000



Authors: V.I. Brake, M.J. Duchesne, K. Dewing, M. Claproot, E. Gougeon, and T.A. Brent
Time-structure map by V.I. Brake and M.J. Duchesne, Geological Survey of Canada, 2013
Depth-structure map by M.J. Duchesne and V.I. Brake, Geological Survey of Canada, 2013
Seismic interpretation by V.I. Brake and M.J. Duchesne, Geological Survey of Canada, 2010–2013

Geomatics by: V.I. Brake, Geological Survey of Canada and G. Huot-Vézina, Institut national de la recherche scientifique
Cartography by: R. Boivin
Scientific editing by: E. Inglis
Initiative of the Geological Survey of Canada, conducted under the auspices of the Western Arctic Islands' project as part of Natural Resources Canada's Geo-mapping for Energy and Minerals (GEM) program.

CANADIAN GEOSCIENCE MAP 163
TIME- AND DEPTH-STRUCTURE MAP
CHRISTOPHER FORMATION
Sabine Peninsula, Melville Island
Nunavut-Northwest Territories
1:200 000

Map projection: Universal Transverse Mercator, zone 12
Base map at the scale of 1:250 000 from Natural Resource Canada, with modifications.
Proximity to the North Magnetic Pole causes the magnetic compass to be useless in this area.
This map is not to be used for navigational purposes.

The Geological Survey of Canada welcomes corrections or additional information from users.
The data may include additional observations not portrayed on this map. See documentation accompanying the data.
This publication is available for free download through GEOCAN (http://geocan.ess.nrcan.gc.ca/).

